ELSEVIER

Water Research 38 (2004) 1003–1013

WATER RESEARCH

www.elsevier.com/locate/watres

Modelling microbial adaptation to changing availability of substrates

Bernd W. Brandt*, Fleur D.L. Kelpin, Ingeborg M.M. van Leeuwen, Sebastiaan A.L.M. Kooijman

Department of Theoretical Biology, Faculty of Earth and Life Sciences, Vrije Universiteit, De Boelelaan 1085, 1081 HV Amsterdam, The Netherlands

Received 23 August 2002; received in revised form 3 September 2003; accepted 19 September 2003

Abstract

In their natural environment microorganisms encounter changes in substrate availability, involving either nutrient concentrations or nutrient types. They have to adapt to the new conditions in order to survive. We present a model for slow microbial adaptation, involving the synthesis of new enzymes, in response to changes in the availability of substitutable substrates. The model is based on reciprocal (or mutual) inhibition of expression of both the substrate-specific carriers and the associated assimilatory machinery. The inhibition kinetics is derived from the kinetics of synthesizing units. An interesting property of the adaptation model is that the presence of a single limiting resource results in a *constant* maximum specific substrate consumption rate for fully adapted microorganisms. Because the maximum specific consumption rate is not a function of substrate concentration, for growth on one substrate, the Monod and Pirt models for instance are still valid. Other adaptation models known to us do not fulfil this property. The simplest version of our model describes adaptation during diauxic growth, using only one preference parameter and one initial condition. The applicability of the model is exemplified by fitting it to published data from diauxic growth experiments.

Keywords: Adaptation; Substrate availability; Simultaneous substrate consumption; Growth; Synthesizing unit; Diauxie

1. Introduction

Many microorganisms are able to grow on a wide variety of substrates, the consumption of the substrates being either sequential or simultaneous. Indeed, sequential utilization resulting in diauxic growth [1] has often been observed. During diauxic growth, depletion of the first substrate is followed by a lag period in which the microorganisms adapt to the second substrate. After this lag phase, exponential growth on the second substrate starts. The length of the intermediate lag period depends on pre-culturing conditions and the relative concentrations of the substrates, as well as on the type of substrates [2].

In the environment many carbon sources are present. This means that heterotrophic microorganisms have the opportunity to utilize several substrates simultaneously. This co-utilization enables microorganisms to attain considerable growth rates, even when each substrate is present at a very low concentration [3]. Moreover, simultaneous substrate consumption is important to the degradation of pollutants present at low concentrations. Furthermore, substrates can be consumed sequentially in batch culture, whereas they are consumed simultaneously in continuous culture or in nature. In a previous article, we formulated a model framework for multiple substrate biodegradation [4] that does not take adaptation into account.

*Corresponding author. Tel.: +31-20-4447005; fax: +31-20-4447123.

E-mail address: bernd@bio.vu.nl (B.W. Brandt).

0043-1354/$ - see front matter
doi:10.1016/j.watres.2003.09.037

Nomenclature

The symbols used for the dimensions are: –, no dimension; t, time; l, length; #, amount (C-mol or mass).

f_i	$S_i/(K_i+S_i)$ (–)
h	enzyme turnover rate (t^{-1})
j_{im}	max. spec. consumption rate of substrate i ($\#\,\#^{-1}\,t^{-1}$)
j_i	specific arrival rate of compound i ($\#\,\#^{-1}\,t^{-1}$)
j_i'	scaled arrival rate of compound i : $j_i' = j_i\rho_i$ ($\#\#^{-1}\,t^{-1}$)
K_i	saturation constant of substrate i ($\#l^{-3}$)
k_i	handling rate for compound i (t^{-1})
k	signal flux proportionality constant ($\#\#^{-1}t^{-1}$)
n_i	number of 'enzymes' i per structural mass ($\#\#^{-1}$)
p_i	preference parameter for adaptation to substrate i (–)
r	biomass growth rate (t^{-1})
r_{max}	maximum biomass growth rate (t^{-1})
S_i	concentration of substrate i ($\#/l^{-3}$)
X	biomass concentration ($\#/l^{-3}$)
y_{ij}	stoichiometric coefficient (coupler): compound i needed per compound j formed ($\#\#^{-1}$)
Y_i	Monod yield factor ($\#\#^{-1}$)
θ_{ij}	fraction of synthesizing units occupied by compound i and j (–)
κ_i	expression fraction of enzyme for substrate i (–)
κ_i°	background expression fraction of substrate i (–)
κ_i^{max}	max. expression fraction of substrate i (–)

In growth models, based on the Monod model, microorganisms consume substrate at a rate that depends hyperbolically on substrate concentration. The maximum specific consumption rate, however, does not depend on the substrate concentration. The parameters that control the uptake process are constant during fast changes of substrate types and availability, but can be subjected to slow adaptation processes that take several generations.

We modelled the slow microbial adaptation of consumption of various substitutable substrates (i.e., substrates that can fulfil the same role in metabolism). We assumed that the pathway for each substrate is inducible and that the presence of one substrate is able to influence the expression of the pathway of other substrates. The article is organized as follows. To start, we introduce binding-inhibition kinetics in a synthesizing unit (SU) framework. Then we use the obtained binding-inhibition equations to describe the expression of a pathway in response to changes in substrate availability. Finally, we develop the adaptation model and confront it with experimental data on diauxic growth.

2. Substrate availability and signal fluxes

Regulatory mechanisms are responsible for adaptation. It is well known that the presence of a substrate induces a signal in the microorganisms that can alter their catabolic properties [5]. Mechanisms involved in the glucose–lactose diauxie in *Escherichia coli* have been known for a long time [5] and we may be tempted to model them in detail. However, it has recently been found that the main reason for the diauxie is inducer exclusion: while glucose is present, lactose is not taken up [6,7]. Furthermore, the mechanisms of carbon catabolite repression differ substantially among bacteria [7]. These differences and changing insights into details of reported mechanisms convinced us to develop an adaptation model that focuses on the general processes rather than on the biochemical details. The model is species independent and, in addition, has the advantage that it requires less parameters and equations than a model that describes the biochemical processes in detail. This is important for practical applications.

We assume that each substrate has a specific regulatory protein that handles the signal fluxes and decides whether to increase or decrease the catabolic capacity for the substrate. The regulatory protein functions as a synthesizing unit (SU) that controls the synthesis of assimilatory machinery for that substrate. An SU is a generalized enzyme that follows classic association–dissociation kinetics with two modifications [8,9]: (i) production fluxes relate to arrival fluxes of substrates at the SU, and (ii) the dissociation rate between substrate and SU is negligibly small. We deal with a metabolic pathway as if we deal with a single rate-limiting enzyme. In sum, the availability of a certain substrate produces a signal flux, handled by an SU. For organisms that are able to adapt, this results in adaptation to a substrate in response to the concentrations of all available substrates.

In this article we derive the adaptation model for two substrates, but the model can easily be extended to account for any number of substrates. When two substrates are present in the medium, two situations are possible. First, the presence of one substrate does not affect the consumption of the other. This situation results from "unilateral binding inhibition." Second, the presence of one substrate can influence the consumption of the other. This situation results from "bilateral

binding inhibition." Both cases of inhibition are treated in detail below using the synthesizing unit concept. The production flux of a certain SU determines the change in the amount of the corresponding rate-limiting enzyme. In this section, we explain how unilateral and bilateral binding inhibition give rise to changing maximum specific substrate consumption rates in response to changing substrate availability. In the next section, we deduce simple equations describing the adaptation process.

2.1. Unilateral binding inhibition

In unilateral binding inhibition, one substrate can repress the utilization of another but not vice versa. We obtain an equation for the synthesis of enzyme that controls the maximum specific uptake rate of a particular substrate. As explained above, we assume that the presence of two substrates (A and B) induces two fluxes of signal molecules ($\tilde{A}$ and $\tilde{B}$). A signal molecule $\tilde{A}$, induced by the presence of substrate A, results in the synthesis of a certain number of enzymes. Fig. 1 depicts the following process. We deal with the reaction $y_{AC}\tilde{A} \rightarrow C$ that is inhibited by compound B. The presence of y_{AC} signal molecules $\tilde{A}$ gives rise to the production of one molecule of enzyme C; thus y_{AC} is a stoichiometric constant. The SU can bind both $\tilde{A}$ and $\tilde{B}$, but it can bind $\tilde{A}$ only if $\tilde{B}$ is not bound. $\tilde{B}$ does not affect the production of C if $\tilde{A}$ is already bound; $\tilde{A}$ does not affect the binding or release of $\tilde{B}$. The SU can be in four different states: unoccupied ($\theta..$), occupied by $\tilde{A}$ only ($\theta_{A}.$), occupied by $\tilde{B}$ only ($\theta_{.B}$), or occupied by both $\tilde{A}$ and $\tilde{B}$ (θ_{AB}).

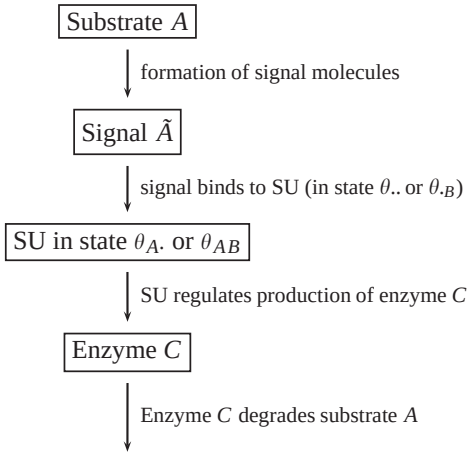

Fig. 1. Sequence of events in the adaptation to substrate A. Substrate A gives rise to signal molecules $\tilde{A}$, which can induce the synthesis of enzymes degrading substrate A. These signal molecules can bind to an SU that regulates the enzyme synthesis of enzyme C. Binding of signals can be inhibited by signal molecules $\tilde{B}$ coming from substrate B.

The equations for the change in the bound fractions of the SU become:

$$\frac{d}{dt}\theta.. = k_A\theta_A. + k_B\theta_{.B} - (j'_A + j'_B)\theta..,$$
$$\frac{d}{dt}\theta_A. = j'_A\theta.. + k_B\theta_{AB} - k_A\theta_A. - j'_B\theta_A.,$$
$$\frac{d}{dt}\theta_{.B} = j'_B\theta.. + k_A\theta_{AB} - k_B\theta_{.B},$$
$$1 = \theta.. + \theta_A. + \theta_{.B} + \theta_{AB},$$

with $j'_i = j_i\rho_i$, where ρ_i is the binding probability and j_i the arrival rate of signal molecules induced by substrate i. The steady-state fractions of bound SUs are $\theta^*_{ij} = \Theta_{ij}/\Theta_+$, with $\Theta_+ = \Theta_{..} + \Theta_{A}. + \Theta_{.B} + \Theta_{AB}$ and

$$\Theta.. = k_Ak_B(j'_B + k_A + k_B),$$
$$\Theta_A. = j'_Ak_B(k_A + k_B),$$
$$\Theta_{.B} = k_Aj'_B(j'_A + j'_B + k_A + k_B),$$
$$\Theta_{AB} = j'_Aj'_Bk_B.$$

The C production flux is given by

$$j_C = y_{CA}k_A(\theta^*_{A}. + \theta^*_{AB})\frac{y_{CA}j'_Ak_Ak_B}{(j'_B + k_B)(k_A + j'_A/(1 + j'_B/k_+))},$$

where $k_+ = k_A + k_B$. The maximum C production flux for $j'_A \rightarrow \infty$ is $j_{C\mathrm{m}} = y_{CA}k_Ak_B(1 + j'_B/k_+)/(j'_B + k_B)$. If $j'_B = 0$, the production reduces to $j_C = y_{CA}j'_Ak_A/(k_A + j'_A)$ as expected from the Michaelis–Menten kinetics. If signal molecule $\tilde{B}$ results in the synthesis of an enzyme D, the D production flux is given by

$$j_D = y_{DB}k_B(\theta^*_{.B} + \theta^*_{AB}) = \frac{y_{DB}j'_Bk_B}{j'_B + k_B}.$$

This formulation of binding inhibition is the simplest. Additional biological details can be introduced, such as binding probabilities or dissociation rates that depend on whether or not the other compound is bound. Although the introduction of such dependencies can allow the description of more complex inhibition patterns, it also implies an increase in the number of parameters.

2.2. Bilateral binding inhibition

In bilateral binding inhibition, one substrate can repress the use of another and vice versa. As above, we deal with the reaction $y_{AC}\tilde{A} \rightarrow C$ that is inhibited by compound B. In addition, we now have the reaction $y_{BD}\tilde{B} \rightarrow D$ that is inhibited by compound A. Again, y_{AC} and y_{BD} are stoichiometric constants, and C and D are the key enzymes involved in processing substrates A and B. In this case, the inhibition is reciprocal. The SU can bind both $\tilde{A}$ and $\tilde{B}$, but it can bind $\tilde{A}$ only if $\tilde{B}$ is not bound, and vice versa. The equations for the change in

the bound fractions of the SU now read:

$$\frac{\mathrm{d}}{\mathrm{d}t}\theta_{..} = k_A\theta_{A.} + k_B\theta_{.B} - (j'_A + j'_B)\theta_{..},$$
$$\frac{\mathrm{d}}{\mathrm{d}t}\theta_{A.} = j'_A\theta_{..} + k_B\theta_{AB} - k_A\theta_{A.},$$
$$\frac{\mathrm{d}}{\mathrm{d}t}\theta_{.B} = j'_B\theta_{..} + k_A\theta_{AB} - k_B\theta_{.B},$$
$$1 = \theta_{..} + \theta_{A.} + \theta_{.B} + \theta_{AB},$$

with $j'_i = j_i\rho_i$, where ρ_i is the binding probability and j_i the arrival rate of signal molecules induced by substrate i. The steady-state fractions of bound SUs are $\theta^*_{ij} = \Theta_{ij}/\Theta_+$, with $\Theta_+ = \Theta_{..} + \Theta_{A.} + \Theta_{.B} + \Theta_{AB}$ and

$$\Theta_{..} = k_Ak_B, \quad \Theta_{A.} = j'_Ak_B, \quad \Theta_{.B} = j'_Bk_A, \quad \Theta_{AB} = 0.$$

The resulting C production flux is given by

$$j_C = y_{CA}k_A\theta^*_{A.} = \frac{y_{CA}j'_Ak_Ak_B}{j'_Ak_B + j'_Bk_A + k_Ak_B}. \tag{1}$$

The maximum flux of C for $j'_A \to \infty$ is $j_{C\mathrm{m}} = y_{CA}k_A$. If $j'_B = 0$, the production reduces to $j_C = y_{CA}j'_Ak_A/(k_A + j'_A)$ as expected. The situation for substrates A and B and their induced production fluxes are now symmetric.

3. Adaptation

3.1. Model development

The production of the key enzymes for the processing of substrates is controlled by signals to the synthesis machinery, while the signals are produced by substrates that are taken up. If enzyme production depends on the magnitude of these signals, the production at varying substrate concentrations varies even when only one substrate is present. In this single substrate situation, the maximum specific consumption rate will become a function of substrate concentration. However, a constant maximum specific consumption rate is usually assumed in popular and successful microbial growth models [1,9–11]. The empirical success of these models leads to the conclusion that the production of assimilation machinery does not respond to the absolute signal size, but to the *relative* signal size (i.e., the signal value is divided by the maximum signal value).

If substrates A and B are processed in parallel and we have n_A assimilatory units for substrate A per unit of structural mass, the substrate processing rate for substrate A is proportional to n_Af_A, where $f_A = S_A/(S_A + K_A)$ with saturation constant K_A and substrate concentration S_A. The signal size is proportional to this flux (with proportionality constant p^*_i), so the relative signal size is $s_A = p^*_An_Af_A/\sum_i p^*_in_if_i$. This formulation allows for a substrate-specific signal amplification via weight coefficients p^*_i, which also accounts for the binding probability of the signal to the signal processing unit (regulatory protein). The signal is actually a flux, so the relative signal flux can be written as s_Ak, where k represents the flux proportionality constant as well as the total signal strength, since $s_A + s_B = 1$. In mathematical terms this means $j'_A = ks_A$ and $j'_B = ks_B$.

The signals are processed in a reciprocal inhibitory way to allow some metabolic memory and preferences for particular substrates. The production rate of assimilatory machinery is proportional to that of the biomass, which has specific growth rate r (see Section 3.3 below). The specific production rate of assimilatory machinery, as defined by Eq. (1), does not depend on the biomass production rate. If the biomass growth rate doubles, the production rate of key enzymes should also double in order to keep the number of assimilatory units per unit of biomass constant. Thus, we multiply the specific production rate by a factor r/r_0, with r_0 some reference rate.

The dilution of assimilatory machinery by growth amounts to $-rn_A$ for substrate A. If the machinery is not restored during exponential growth, it will dilute in the newly formed biomass in an exponential way. In sum

$$\frac{\mathrm{d}}{\mathrm{d}t}n_A = j_C\frac{r}{r_0} - rn_A. \tag{2}$$

In this equation, we make a quasi-steady-state assumption for j_C on the basis of time-scale arguments, as is customary, since enzyme kinetics is faster than growth kinetics.

Using bilateral binding inhibition (Eq. (1)), the change in the amount of rate-limiting machinery for substrate A is now given by

$$\frac{\mathrm{d}}{\mathrm{d}t}n_A = r\left(\frac{n^*_As_A(1 + k/k_A)}{s_A(1 + k/k_A) + s_B(1 + k/k_B)} - n_A\right),$$

where $n^*_A = (y_{CA}k/r_0)/(1 + k/k_A)$ is the steady-state rate-limiting enzyme concentration for substrate A for exposure to that substrate only.

The expression fraction is defined as $\kappa_i = n_i/n^*_i$. As it represents the ratio of the expression and the maximum attainable expression (n^*_i), it has a value between zero and one. From the equation above the change in these fractions is given by

$$\frac{\mathrm{d}}{\mathrm{d}t}\kappa_A = r\left(\frac{p_A\kappa_Af_A}{p_A\kappa_Af_A + p_B\kappa_Bf_B} - \kappa_A\right),$$
$$\frac{\mathrm{d}}{\mathrm{d}t}\kappa_B = r\left(\frac{p_B\kappa_Bf_B}{p_A\kappa_Af_A + p_B\kappa_Bf_B} - \kappa_B\right), \tag{3}$$

where $p_i = p^*_in^*_i(1 + k/k_i)$ are substrate preference coefficients. Without loss of generality, we can take $p_A + p_B = p_+ = 1$. Please note that for $\kappa_+ = \kappa_A + \kappa_B$, we have $\mathrm{d}\kappa_+/\mathrm{d}t = r(1 - \kappa_+)$, which gives the natural constraint $\kappa_A(0) + \kappa_B(0) = 1$ on the initial conditions. Once $\kappa_A(t) + \kappa_B(t) = 1$ for some value of time t, it remains one at all time points. These constraints reduce the system above

to a single equation with effectively two parameters, p_A and $\kappa_A(0)$.

3.2. Model analysis

Prolonged exposure to substrate A only ($f_B = 0$) results in maximum expression ($\kappa_A \to 1$) of the corresponding rate-limiting enzyme, whereas prolonged absence of substrate A ($f_A = 0$) results in no expression at all ($\kappa_A \to 0$). For constant substrate concentrations, the expression is either maximum or zero at steady state, depending on which value for $p_i f_i$ is the largest. In a steady-state chemostat, dual substrate consumption can take place, since the microorganism adapts until $p_A f_A = p_B f_B$.

If the organisms have depleted their own substrates, the final values of the expression fractions depend on how the substrates were depleted. This is because the adaptation rate is linked to the growth rate (cf. Eqs. (2) and (3)). After complete depletion of the resources the adaptation equations above become mathematically undetermined. In the unlikely situation that this behaviour poses a problem in a practical application, it can be avoided by adding a background signal for each substrate and replacing f_i by $f_i + \varepsilon_i$ for $i = A, B$.

When a particular substrate has been absent for a very long period its expression fraction becomes zero. The microorganism then is not able to initiate the uptake of that substrate. Since this behaviour is asymptotic only, it will probably not constitute a problem in practice. Moreover, it can be avoided by adding a small background signal as above or by introducing a background production flux as rk_i° for $i = A, B$. As a consequence of the addition of the background production flux, the maximum value of κ_i will no longer be one. Substrate uptake now becomes $\mathrm{d}S_i/\mathrm{d}t = -(\kappa_i/\kappa_i^{\max}) f_i X$, where $\kappa_i^{\max} = 1 + \kappa_i^\circ$ represents the maximum value of the expression fraction κ_i.

The assimilation machinery, including the carriers, are part of cells' structure. Cells maintain their structure by degrading and reconstructing their functional proteins. Such enzyme-specific maintenance becomes visible in the adaptation process as a protein decay and an enhanced synthesis via term h. Incorporation of this enzyme turnover into the adaptation model, for an arbitrary number of substrates, leads to

$$\frac{\mathrm{d}}{\mathrm{d}t}\kappa_i = (r+h)\left(\frac{p_i\kappa_i f_A}{\sum_j p_j \kappa_j f_j} + \kappa_i^\circ - \kappa_i\right), \tag{4}$$

with $\sum_i p_i = 1$. Notice that for $\kappa_+ = \sum_i \kappa_i$ and $\kappa_+^\circ = \sum_i \kappa_i^\circ$ we have

$$\frac{\mathrm{d}}{\mathrm{d}t}\kappa_+ = (r+h)(1 + \kappa_+^\circ - \kappa_+),$$

which implies that as soon as $\kappa_+(t) = 1 + \kappa_+^\circ$, it will never leave this value. This can be used as a constraint on the initial conditions for κ_i to remove one degree of freedom from the system.

Our adaptation model spans the full range of nutrient utilization, from simultaneous substrate consumption to sequential consumption. For two nutrients, the mode of consumption depends on the value of a single preference parameter (p_A); if it is very small, substrate B will be taken up first. Notice that we also have initial conditions for the expression fractions, which count as parameters in fits to experimental data, although their significance vanishes in time. The model can be extended in several ways, for example by accounting for cross-competitive inhibition between the substrates or for unilateral binding inhibition.

A very important feature of this model for adaptation is that once the cells are adapted, cell growth and substrate uptake are "normal" again. This means that the adaptation module can easily be combined with other modules, such as the Monod model [1], the Herbert–Marr–Pirt models [10,12,13], the Droop model [11] or the DEB model [9]. The crucial property is that the substrate availability and the growth rate do not influence the number of carriers (or level of key enzymes) of fully adapted organisms. Alternative models that are known to us [14–16] do not satisfy this property. This implies that the adaptation process as described by these models affects the dynamics of fully adapted cells, which seems unrealistic to us.

3.3. Biomass growth

Although the equations in the previous section fully specify substrate uptake, they do not yet specify the biomass growth process itself. However, as we stated before, the adaptation model has the advantage that it can be combined with any microbial growth model. Hence, the Monod model [1] can be used. If, in addition, we know the maintenance requirements of the microorganism, Pirt's model [10] can be used. Alternatively, the DEB model [9] can be used. This is a more elaborate and realistic growth model that accounts for the presence of reserves. For more information about the DEB model we refer the reader to the Appendix.

For any of the growth models cited in this article, the consumption rate of substrate i and the biomass growth rate are given by

$$\frac{\mathrm{d}}{\mathrm{d}t}S_i = -j_{\mathrm{im}}\frac{\kappa_{\mathrm{i}}}{\kappa_{\mathrm{i}}^{\max}}\frac{S_i}{S_i + K_i}X, \tag{5}$$

$$\frac{\mathrm{d}}{\mathrm{d}t}X = rX, \tag{6}$$

with maximum specific uptake rate j_{im} and biomass concentration X. The change in the expression fractions are given by Eq. (4). In case of zero background expression, $\kappa_{\mathrm{i}}^{\max}$ is equal to one. The expression for the

specific growth rate r varies from one model to another. In the Monod model, for example, the yield factor Y_i relates substrate consumption to biomass growth: $r = (1/X)\sum_i Y_i(\mathrm{d}S_i/\mathrm{d}t)$.

3.4. Model equations

In the following sections we use the adaptation model, in combination with the Monod model, in simulations and in data fitting. We assume that background expression is absent (thus $\kappa_i^{\max} = 1$). For two substrates, the set of differential equations describing adaptation: is

$$\frac{\mathrm{d}}{\mathrm{d}t}X = rX,$$
$$\frac{\mathrm{d}}{\mathrm{d}t}S_A = \frac{r_{A\,\max}}{Y_A}\kappa_A f_A X,$$
$$\frac{\mathrm{d}}{\mathrm{d}t}S_B = \frac{r_{B\,\max}}{Y_B}\kappa_B f_B X,$$
$$\frac{\mathrm{d}}{\mathrm{d}t}\kappa_A = (r+h)\left(\frac{\kappa_A f_A}{\kappa_A f_A + w\kappa_B f_B} - \kappa_A\right),$$
$$\frac{\mathrm{d}}{\mathrm{d}t}\kappa_B = (r+h)\left(\frac{\kappa_B f_B}{\kappa_A f_A/w + \kappa_B f_B} - \kappa_B\right),$$

where

$$f_A = \frac{S_A}{S_A + K_A}, \quad f_B = \frac{S_B}{S_B + K_B},$$
$$w = p_B/p_A,$$
$$r = \kappa_A r_{A\,\max} f_A + \kappa_B r_{B\,\max} f_B.$$

The adaptation module has only three parameters: $h, p_A/p_B$, and $\kappa_A(0)$. Please note that the last parameter is an initial condition and not an adaptation-process-related parameter. Remember that $\kappa_B(0) = 1 - \kappa_A(0)$. The Monod model for two substrates has nine parameters: $r_{i\,\max}, Y_i, K_i, S_i(0)$, for $i = A, B$, and $X(0)$. The parameters $S_i(0)$ and X(0) are initial conditions, whereas $r_{i\,\max}$, Y_i, and K_i are Monod growth parameters.

Below we show model simulations in which we assigned values to the parameters. Thereafter, we apply the model to data. For the parameter estimation procedure, we assumed constant variance with no covariance for the observations (least-squares regression).

4. Model simulation

A model simulation reveals the influence of the preference parameters p_i, and adaptation, on the diauxic lag and on the substrate consumption. We carried out the simulations below by numerically solving the set of differential equations above. We assigned the values obtained in [14] (Table 1) to the Monod growth parameters, whereas we gave representative values to the remaining parameters.

Table 1
Monod parameter values of *Klebsiella oxytoca* obtained in [14] from single substrate growth data. The maximum growth rate $r_{\max}$, the saturation constant K, and the yield factor Y are given.

Carbon source	$r_{\max}$ (h^{-1})	K(g/L)	Y (g dry wt/g)
Glucose (A)	1.08	0.01	0.52
Xylose (B)	0.82	0.2	0.50

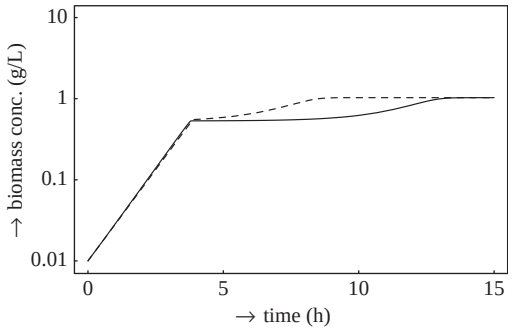

Fig. 2. Influence of the preference parameter p_A on the length of the lag phase. The figure shows growth on two carbon sources with different preference parameter values ($p_B/p_A = 0.1$, solid line; $p_B/p_A = 0.1$, dashed line). When the microorganisms prefer the first substrate to the second substrate ($p_B/p_A = 0.1$), the length of the diauxic lag increases (parameter values from Table 1). Adaptation-model parameters: $h = 0.0\,h^{-1}$, $p_B/p_A = 0.1$ or $p_B/p_A = 1.0$. Initial conditions: $S_A(0) = 1.0$ g/L, $X(0) = 0.01$ g dry wt/L, $\kappa_A(0) = 0.90$.

Fig. 2 illustrates the influence of substrate preference on the lag phase. In this simulation, the microorganisms have the same preference for both substrates or a ten times higher preference for the first, respectively. A higher preference for the first substrate results in a longer lag phase before growth on the second starts. The initial value of the expression fraction $\kappa_A(0)$ was set to 0.90, which means that the biomass is 90% adapted to substrate A.

Fig. 3 shows the result of adaptation for a steady-state continuous culture. The expression fractions as well as the resulting steady-state biomass and substrate concentrations are shown as a function of the dilution rate. Experimental results show that at low dilution rates both substrates are consumed, whereas at high dilution rate only one substrate is consumed, cf. [3,15,17]. As can be seen from Fig. 3, this is also predicted by the adaptation model. We remark that, in experiments by Lendenmann et al. *E. coli* used all sugars in different mixtures simultaneously, independent of mixture composition and dilution rate [18]. However, this is not necessarily in disagreement with our prediction as it can be due to the types of sugars and the range of dilution rates used.

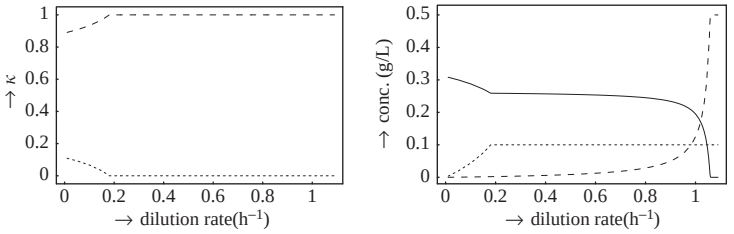

Fig. 3. Influence of the dilution rate on the expression fractions and substrate concentrations in a steady-state chemostat with input concentrations of 0.5 g/L substrate A (dashed line) and 0.1 g/L substrate B (dotted line). Left: the expression fractions as a function of the dilution rate. Right: the substrate concentrations and biomass (solid line) concentration as a function of the dilution rate (parameter values from Table 1). Adaptation-model parameters: $h = 0.0\,\mathrm{h}^{-1}$, $p_B/p_A = 0.5$.

5. Applications

In this section we use the model to describe data from the literature, starting with the growth of *Klebsiella oxytoca* on glucose and xylose [14]. A second example is the diauxic growth of *Pseudomonas oxalaticus* on acetate and oxalate [19]. A third example is the diauxic growth on fructose and succinate [20].

5.1. Diauxic growth on glucose and xylose

Kompala et al. [14] have reported the diauxic growth of *Klebsiella oxytoca* on, for example, glucose and xylose. We applied our model to their data, using the Monod model for growth. During the estimation process the Monod parameters remain fixed on the values given in Table 1. We show a series of model validations followed by a model prediction. In this example, the values of the turnover parameter (h) must be identical for all fits. The values of the adaptation parameters and the values of the initial biomass concentrations have been estimated. We used the measured initial substrate concentrations in Figs. 6–8. Initial substrate concentrations in Figs. 4 and 5 were estimated separately by using the values of the Monod parameters (Table 1), since [14] does not report them. Note that the value of the preference parameter p_B/p_A is not relevant for the growth on one substrate. In the following figures the dots represent the experimental data and the lines the model calculations.

Figs. 4 and 5 show fits to data on the growth on either glucose or xylose of an inoculum pre-cultured on glucose. Figs. 6 and 7 show fits to the data on glucose–xylose diauxie. These data refer to an inoculum pre-cultured on glucose and an inoculum pre-cultured on xylose, respectively. Fig. 8 shows a model prediction using the parameter values obtained by fitting the data shown in Figs. 4–7. Although none of the model parameters were fitted to this data-set, the predicted behaviour corresponds with the experimental results. The parameters used in these figures are as follows. The adaptation parameters are $h = 0.67\,\mathrm{h}^{-1}$, $p_B/p_A = 0.68$. The Monod parameter values are shown in Table 1. The initial conditions are given in the figures' legends.

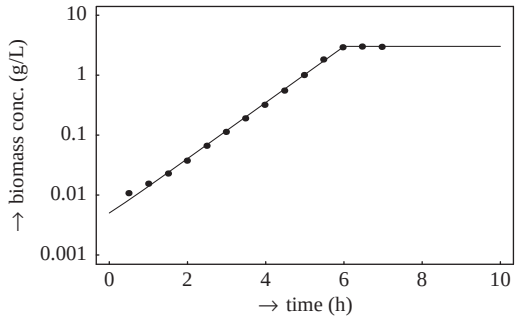

Fig. 4. Model validation of growth of *K. oxytoca* on glucose after pre-culturing on glucose. The dots represent experimental data (from [14]), the line represents the model fit. Adaptation parameters: $h = 0.67\,\mathrm{h}^{-1}$, $p_B/p_A = 0.68$. Monod parameter values from Table 1. Initial conditions: $S_A(0) = 5.8$ g glucose/L, $X(0) = 0.005$ g dry wt/L, $\kappa_A(0) = 0.89$.

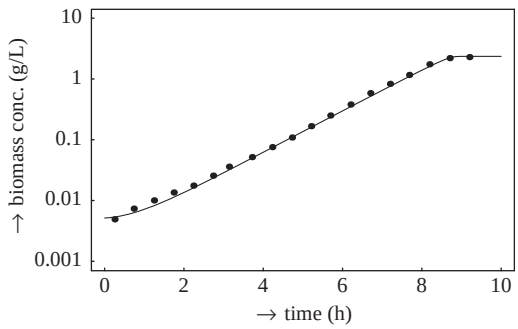

Fig. 5. Model validation of growth of *K. oxytoca* on xylose after pre-culturing on glucose. The dots represent experimental data (from [14]), the line represents the model fit. Growth and adaptation parameters as in Fig. 4. Initial conditions: $S_B(0) = 4.7$ g xylose/L, $X(0) = 0.0051$ g dry wt/L, $\kappa_B(0) = 0.11$.

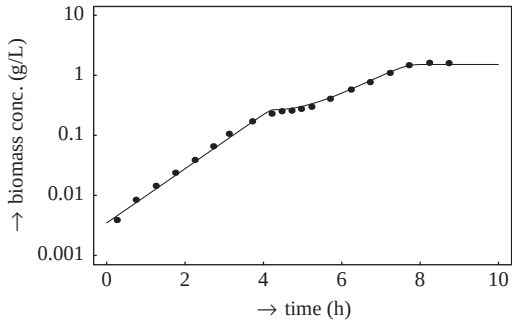

Fig. 6. Model validation of growth of *K. oxytoca* on glucose and xylose after pre-culturing on glucose. The dots represent experimental data (from [14]), the line represents the model fit. Growth and adaptation parameters as in Fig. 4. Initial conditions: $S_A(0) = 0.5$ g glucose/L, $S_B(0) = 2.5$ g xylose/L, $X(0) = 0.035$ g dry wt/L, $\kappa_A(0) = 0.89$, $\kappa_B(0) = 0.11$.

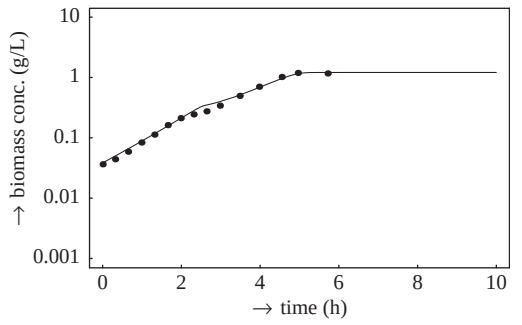

Fig. 7. Model validation of growth of *K. oxytoca* on glucose and xylose after pre-culturing on xylose. The dots represent experimental data (from [14]), the line represents the model fit. Growth and adaptation parameters as in Fig. 4. Initial conditions: $S_A(0) = 0.33$ g glucose/L, $S_B(0) = 2.0$ g xylose/L, $X(0) = 0.038$ g dry wt/L, $\kappa_A(0) = 0.23$, $\kappa_B(0) = 0.77$.

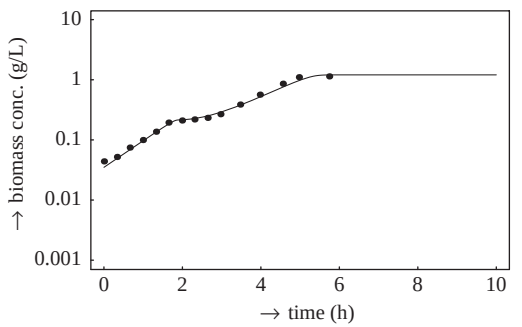

Fig. 8. Model prediction of growth of *K. oxytoca* on glucose and xylose after pre-culturing on glucose. The dots represent experimental data (from [14]), the line represents the model fit. Growth and adaptation parameters as in Fig. 4. Initial conditions: $S_A(0) = 0.33$ g glucose/L, $S_B(0) = 2.0$ g xylose/L, $X(0) = 0.035$ g dry wt/L.

5.2. Diauxic growth on acetate and oxalate

Dijkhuizen et al. [19] have reported the diauxic growth of *Pseudomonas oxalaticus* OX1 on acetate and oxalate. To fit our model to this data set, we set the initial condition of substrate and biomass concentration to the measured values at time zero. Furthermore, we fixed the value of the saturation constants on 0.01 mM, because the data do not contain information to estimate these constants well. The estimated values for the other parameters are given in Fig. 9. The estimated values for the maximum growth rates and yields are within the range values expected under these conditions. The doubling times on acetate and oxalate are usually about 1.8 and 3.6 h, respectively [19]. Fig. 9 depicts a fit of the adaptation model to their data. As can be seen from this figure, the model fits the data well.

5.3. Diauxic growth on fructose and succinate

Azospirillum brasilense has shown diauxic growth when incubated with succinate and fructose [20]. To obtain a model fit of the experimental results, we use our adaptation model in combination with the Monod model. The substrates have been radioactively labelled and their consumption as well as their incorporation into biomass have been measured in three experiments. In the model fit shown below, we used a biomass incorporation percentage of 20% for succinate [20] and of 50% for fructose.

Since radioactivity has been measured, a background radioactivity signal exists during the experiment ($^{14}CO_2$, radioactive products). This means that the substrate concentration based on radioactivity is not zero when all

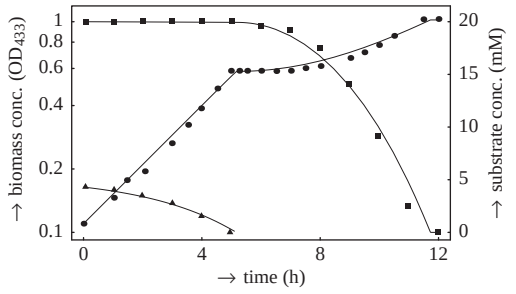

Fig. 9. Model fit to data on growth of *P. oxalaticus* (●) on acetate (■) and oxalate (▲) after preculturing on acetate (data from [19]). Under the experimental conditions, 1 unit optical density (433 nm) is approximately equivalent to 235 mg dry wt/L. Parameter values: $r_{A\max} = 0.33\,h^{-1}$, $r_{B\max} = 0.19\,h^{-1}$, $Y_A = 0.11$ mM acetate OD^{-1}, $Y_B = 0.022$ mM oxalate OD^{-1}, $K_A = 0.01$ mM (fixed), $K_B = 0.01$ mM (fixed), $h = 0.15\,h^{-1}$, $p_B/p_A = 0.5$. Initial conditions: $S_A(0) = D$ 4.3 mM acetate, $S_B(0) = 20$ mM oxalate, $X(0) = 0.11$ OD, $\kappa_A(0) = 0.99$, $\kappa_B(0) = 0.01$.

(primary) substrate has been consumed. The signal of these radioactive products can be incorporated into the model expression for fructose consumption. The formation of radioactive products equals $dP/dt = -\alpha(dS_B/dt) - k_d P$. Since we used an incorporation percentage of fructose of 50%, the parameter α has a value of 0.50. Fig. 10 shows the model fit of fructose disappearance without (solid line) and with (dotted line) the incorporation background radioactivity. The adaptation model fits quite well when we keep in mind that: (i) the data comes from three separate experiments and (ii) during fructose metabolism, an unknown amount of organic acids is produced causing the disappearance of radioactivity to lag behind the consumption of fructose itself.

We remark that, in the uptake experiment, the total consumption rate of fructose remained constant for one to two generations after the addition of succinate to a culture growing on fructose [20]. This can be explained by an immediate and complete stop of the synthesis of fructose degrading key enzymes. At the moment we have not further investigated this immediate change in enzyme synthesis, since the specific fructose consumption rate in the uptake experiment was about 8 times lower than in the corresponding growth experiment. This means that the cells behaved differently in the growth and uptake experiments, possibly due to the harvesting and washing processes.

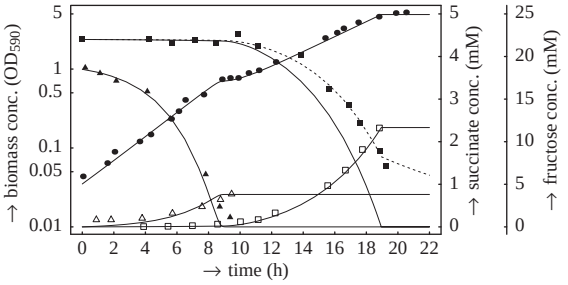

Fig. 10. Model fit of growth of *A. brasilense* on fructose and succinate after pre-culturing on succinate. The data come from three separate experiments [20]: one measures [1,4-^{14}C] succinate in supernatant (▲) and cells (△), one measures D–[U-^{14}C] fructose in supernatant (■) and cells (□), and another measures growth (●). The dotted line indicates the model fit of fructose consumption when the formation of radioactive products from fructose is included ($\alpha = 0.50$, $k_d = 0.1$). One unit of OD_{590} corresponds to 470 μg dry wt/mL. Parameter values: $Y_A = 80.6$ g dry wt/mmol succinate, $Y_B = 90.6$ g dry wt/mmol fructose, $r_{A\max} = 0.38\,h^{-1}$ [20], $r_{B\max} = 0.22\,h^{-1}$ [20], $K_A = 0.1$ mM (fixed), $K_B = 10^{-4}$ mM (fixed), $h = 0.7$, $p_B/p_A = 0.8$. Initial conditions: $S_A(0) = 3.7$ mM succinate, $S_B(0) = 22$ mM fructose, $X(0) = 16.5$ g dry wt/L, $\kappa_A(0) = 0.80$, $\kappa_B(0) = 0.20$.

6. Discussion

The adaptation model presented in this article fits and predicts data on diauxic growth well. At low dilution rates, our model predicts that simultaneous consumption of substrates takes place, whereas at high dilution rates it predicts that only one substrate is consumed. This is in agreement with the experimental observations. Although we illustrated the use of our model with data from diauxic batch experiments, the model can also be used for continuous cultures. For an alternative approach to modelling growth on mixtures in chemostats we refer the reader to [17].

The approach presented in this article differs from previous approaches, as cybernetic modelling (e.g. [14,15]), on some important aspects, which are discussed below.

The description of the adaptation process was obtained by assuming a general regulatory mechanism where the presence of one nutrient can inhibit the utilization of another. This approach has the advantage that it is species independent and parameter sparse. In its simplest version, it describes the adaptation process during diauxic growth with only two parameters: $\kappa_A(0)$ and p_A. A single parameter p_A describes substrate preference during diauxic growth.

In the case of adaptation to a single nutrient, our model predicts a constant maximum key-enzyme level. Thus, the maximum specific consumption rate is always a constant, irrespective of enzyme decay and substrate concentration. Our model differs in this aspect from other adaptation models. Such a constant maximum rate is the basis of most growth models (Monod, Pirt, Droop, DEB [9]). Moreover, it is difficult to know beforehand whether key enzymes for a certain substrate are inducible. Therefore, the application of models for adaptation that do not assume this maximum specific consumption rate to be constant (e.g. [14,16]) is problematic in the situation where growth on a single substrate is quantified. The level of key enzyme and, therefore, the maximum specific consumption rate remains a function of substrate concentration in these models. If a Monod model has successfully been applied to single-substrate situations, but later research reveals that key enzymes are inducible, this implies that earlier work must be redone. Contrary to other adaptation models known to us [14–16], our adaptation model does not suffer from this problem even when enzyme decay occurs. If enzyme decay does not take place, the other models also simplify to a Monod model, since the relative enzyme level $(e/e_{\max})$ is then independent of the substrate concentration. For a single substrate situation the current adaptation model simplifies exactly to the growth model for cells in steady state. During steady-state growth on a single substrate, the influence of the adaptation process on substrate consumption is absent.

Furthermore, we did not introduce optimal control into the adaptation model a priori; bacteria may optimize total biomass, or growth rate [2,15], or possibly something else. No introduction of optimal control implies that we do not use this method to reduce the number of parameters, as has been done in the cybernetic approaches [14,15]. However, optimal control can be incorporated into the model. The binding probabilities (see p.3, Section 2.1), for example, can be a function of an optimal control regime.

We point out that this adaptation model primarily describes slow adaptation taking several cell cycles. It is based on the regulation of the synthesis of key enzymes. When a microorganism adapted to substrate A, is transferred to another substrate, the key enzymes for the use of A can be inhibited. This inhibition typically occurs in a time frame of seconds, and can be called fast adaptation. It can be included in this model with, for example, an expression for instantaneous inhibition (see Appendix).

We developed a slow adaptation model based on the interaction and inhibition of substrates during enzyme synthesis. The model was applied to data from diauxic growth experiments, but can be applied to growth on more than two substrates as well. Moreover, it can be extended to account for different processes as enzyme inhibition and can even be used with optimal control without altering the structure of the model.

Acknowledgements

The authors thank Paul Doucet and Bob Kooi for insightful comments. This research is supported by the Technology Foundation STW, applied science division of NWO and the technology programme of the Ministry of Economic Affairs.

Appendix A

A.1. Adaptation with the DEB model

Our adaptation model can be combined with different biomass growth models. In this article we showed how our adaptation model can be applied in combination with the Monod model. Another biomass growth model that can be used is the dynamic energy budget (DEB) model [9], which accounts for reserve dynamics. The main feature of this model is that substrates are assimilated into reserves from which growth costs and maintenance costs are paid. Since in the DEB model, biomass is divided into two compartments, structure and reserves, the biomass composition becomes a function of the growth rate, as has been observed in practice. When the maintenance is negligible and reserve turnover is very fast, the DEB model simplifies to the Monod model. For a thorough introduction to the DEB model we refer the reader to [9,21]. In batch reactors, the DEB biomass growth model in combination with our adaptation model (Eq. (3) or Eq. (4)) results in the following equations:

$$r = \frac{k_{\mathrm{E}} m_{\mathrm{E}} - k_{\mathrm{M}} y_{\mathrm{EV}}}{m_{\mathrm{E}} + y_{\mathrm{EV}}}, \tag{A.1a}$$

$$\frac{\mathrm{d}}{\mathrm{d}t} m_{\mathrm{E}} = \sum_i j_{\mathrm{im}} \frac{\kappa_i}{\kappa_i^{\max}} y_{\mathrm{ES}i} \frac{S_i}{K_i + S_i} - k_{\mathrm{E}} m_E, \tag{A.1b}$$

$$W(t) = w_{\mathrm{V}} X + w_{\mathrm{E}} m_{\mathrm{E}} X. \tag{A.1c}$$

The expression for the substrate consumption (Eq. (5)) also applies to the DEB model; j_{im} is the maximum structural-biomass specific consumption rate of substrate i (C-mol C-mol^{-1} h^{-1}). The growth of structural biomass (X) is defined by Eqs. (6) and (A.1a). Here, the reserve density of limiting nutrient, m_{E}(C-mol/C-mol), comes into play. The higher the reserve density, the higher the growth rate. k_{E} is the reserve turnover rate (h^{-1}) and y_{EV} refers to the amount of reserves needed per amount of structural biomass formed (C-mol/C-mol). For simplicity, we assumed the costs for growth (y_{EV}) remain constant. This means that the costs for key-enzyme synthesis for cells fully adapted to one substrate are the same irrespective of the type of substrate. Maintenance is introduced by the maintenance rate coefficient, k_{M}(h^{-1}). Reserves are replenished by substrate consumption (Eq. A.1b). The efficiency of this process is defined by $y_{\mathrm{E}}\hat{S}_i$ (C-mol/C-mol); the amount of reserves formed per amount of substrate consumed. The total weight (W) of the biomass equals the sum of the weight of reserves and structural biomass (Eq. A.1c). Please note that the Monod model is a special case of the DEB model for $k_{\mathrm{E}} \to \infty$ and $k_{\mathrm{M}} = 0$.

More information about the DEB research programme can be found at http://www.bio.vu.nl/thb/deb/. The adaptation model that is discussed in this article is coded in the package DEBtool, which can be downloaded from the electronic DEB laboratory.

A.2. Fast adaptation

Fast adaptation, or repression of enzyme activity, can also be modelled with bilateral binding inhibition (Eq. (1)). In this case, not the synthesis machinery but the enzyme activity is repressed. Substrate consumption with instantaneous inhibition becomes

$$\begin{aligned}\frac{\mathrm{d}S_A}{\mathrm{d}t} &= -j_{A\mathrm{m}} \frac{j'_A k_B}{j'_A k_B + j'_B k_A + k_A k_B} X \\ &= -j_{A\mathrm{m}} \frac{K_A^{-1} S_A}{K_A^{-1} S_A + K_{BA}^{-1} S_B + 1} X.\end{aligned}$$

The arrival flux j'_A of substrate A at the carrier (or key enzyme) is proportional to the substrate concentration and equals $\alpha_A \rho_A S_A$, where ρ_A is the binding probability. The saturation constant K_A is $k_A/(\alpha_A \rho_A)$. The influence of substrate B on the consumption of A appears in the denominator as $K_{BA}^{-1} S_B$.

References

[1] Monod J. Recherches sur la croissance des cultures bactériennes. 2nd ed. Paris: Hermann; 1958. Thèse de 1942.

[2] Harder W, Dijkhuizen L. Strategies of mixed substrate utilization in microorganisms. Philos Trans R Soc London Ser B 1982;297:459–80.

[3] Egli T. The ecological and physiological significance of the growth of heterotrophic microorganisms with mixtures of substrates. Adv Microb Ecol 1995;14:305–86.

[4] Brandt BW, van Leeuwen IMM, Kooijman SALM. A general model for multiple substrate biodegradation. Application to co-metabolism of structurally non analogous compounds. Water Res 2003;37:4843–54.

[5] Stryer L. Biochemistry, 4th ed. New York: Freeman; 1995.

[6] Kimata K, Takahashi H, Inada T, Postma P, Aiba H. cAMP receptor protein-cAMP plays a crucial role in glucose–lactose diauxie by activating the major glucose transporter gene in *E. coli*. Proc Nat Acad Sci USA 1997;94:12914–9.

[7] Stülke J, Hillen W. Carbon catabolite repression in bacteria. Curr Opin Microbiol 1999;2:195–201.

[8] Kooijman SALM. The synthesizing unit as model for the stoichiometric fusion and branching of metabolic fluxes. Biophys Chem 1998;73:179–88.

[9] Kooijman SALM. Dynamic energy and mass budgets in biological systems, 2nd ed. Cambridge: Cambridge University Press; 2000.

[10] Pirt SJ. The maintenance energy of bacteria in growing cultures. Proc R Soc Lond B Biol Sci 1965;163:224–31.

[11] Droop MR. The nutrient status of algal cells in batch culture. J Mar Biol Assoc UK 1975;55:541–55.

[12] Herbert D. Some principles of continuous culture. In: Tunevall G, editor. Recent progress in micro-biology. Stockholm: Almquist & Wiksell; 1958. p. 381–96.

[13] Marr AG, Nilson EH, Clark DJ. The maintenance requirement of *E. coli*. Ann N Y Acad Sci 1963;102: 536–48.

[14] Kompala DS, Ramkrishna D, Jansen NB, Tsao GT. Investigation of bacterial growth on mixed substrates: experimental evaluation of cybernetic models. Biotechnol Bioeng 1986;28:1044–55.

[15] Kompala DS, Ramkrishna D, Tsao GT. Cybernetic modeling of microbial growth on multiple substrates. Biotechnol Bioeng 1984;26:1272–81.

[16] Liu PH, Svoronos SA, Koopman B. Experimental and modeling study of diauxic lag of *Pseudomonas denitrificans* switching from oxic to anoxic conditions. Biotechnol Bioeng 1998;60:649–55.

[17] Narang A. The steady-state of microbial growth on mixtures of substitutable substrates in a chemostat. J Theoret Biol 1998;190:241–61.

[18] Lendenmann U, Snozzi M, Egli T. Kinetics of the simultaneous utilization of sugar mixtures by *E. coli* in continuous culture. Appl Environ Microbiol 1996;62:1493–9.

[19] Dijkhuizen L, van der Werf B, Harder W. Metabolic regulation in *Pseudomonas oxalaticus* OX1. Diauxic growth on mixtures of oxalate and formate or acetate. Arch Microbiol 1980;124:261–8.

[20] Mukherjee A, Ghosh S. Regulation of fructose uptake and catabolism by succinate in *Azospirillum brasilense*. J Bacteriol 1987;169:4361–7.

[21] Kooijman SALM. Quantitative aspects of metabolic organization; a discussion of concepts. Philos Trans R Soc London Ser B 2001;356:331–49.